4

Cell and Tissue Microdissection in Combination with Genomic and Proteomic Applications

STEPHEN D. GINSBERG, SCOTT E. HEMBY, ELLIOTT J. MUFSON, and LEE J. MARTIN

STEPHEN D. GINSBERG • Center for Dementia Research, Nathan Kline Institute, and Departments of Psychiatry and Physiology and Neuroscience, New York University School of Medicine, Orangeburg, NY 10962 SCOTT E. HEMBY • Department of Physiology and Pharmacology, Wake Forest University School of Medicine, Winston-Salem, NC 27157 ELLIOTT J. MUFSON • Department of Neurological Sciences, Rush University Medical Center, Chicago, IL 60612 LEE J. MARTIN • Division of Neuropathology, Departments of Pathology and Neuroscience, Johns Hopkins University School of Medicine, Baltimore, MD 21205

Abstract: The combination of tissue microdissection protocols including discrete cell microaspiration and laser capture microdissection with high throughput gene expression profiling platforms such as cDNA microarrays and oligonucleotide microarrays enables the simultaneous assessment of many individual elements from a single cell or a population of homogeneous cells. This chapter outlines in detail the theoretical and practical background for selecting the appropriate tissues and conditions amenable to expression profiling. In addition, this report illustrates the usage of microdissection strategies and RNA amplification methodologies in concert with array technologies using tissues harvested from the central nervous system obtained from animal models of neurodegeneration and postmortem human brain tissues.

Keywords: brain, expression profiling, laser capture microdissection, microarray, molecular fingerprint, RNA amplification, SELDI-TOF

I. INTRODUCTION

The brain is a complex structure with heterogeneous neuronal (e.g., pyramidal neurons and interneurons) and nonneuronal (e.g., glial cells, epithelial cells, and vascular elements) cell populations. Advances in molecular biology provide the tools needed to sample gene expression from specific homogeneous cell populations within defined brain regions without potential contamination of adjacent neuronal subtypes and nonneuronal cells, and are an important goal of twenty-first century neuroscience. However, gene expression profiling of homogeneous populations of cells is a difficult task that demands a multidisciplinary approach including molecular biology, cell biology, neuroanatomy, and biomedical engineering. Individual cell types are likely to have unique patterns or a mosaic of gene and protein expression under normative conditions that is likely to be altered in pathological states. For example, distinct cortical and subcortical regions may serve entirely different functions and may be differentially affected in neurodegenerative diseases (Galvin, 2004; Ginsberg *et al.*, 1999b). Indeed, the molecular basis of why certain neuronal cell populations are vulnerable to neurodegeneration, often termed "selective vulnerability," can be elucidated by discrete cell analysis more readily than by utilizing regional and total brain preparations (Ginsberg and Che, 2005). Thus, the pattern

of genomic and proteomic expression in a subpopulation of homogeneous cells or single cells is more likely to be informative than the pattern in a whole tissue homogenate, assuming the target population is well defined. With the advent of modern molecular and cellular techniques, it is now possible to isolate and study genomic DNA, RNA species, and proteins from microdissected tissue sources. At present, an optimal methodology is to evaluate single cells, identified either physiologically in living preparations (Eberwine *et al.*, 1992; Tkatch *et al.*, 2000) or by immunocytochemical or histochemical procedures in fixed cells in vitro or in vivo (Galvin and Ginsberg, 2004; Ginsberg and Che, 2004; Ginsberg *et al.*, 2004; Hemby *et al.*, 2003; Kamme *et al.*, 2003; Mufson *et al.*, 2002; Van Deerlin *et al.*, 2002). Unfortunately, the quantity of RNA harvested from a single cell, estimated to be ~0.1–1.0 pg, is not sufficient for standard RNA extraction procedures (Phillips and Eberwine, 1996; Sambrook and Russell, 2001). Both exponential polymerase chain reaction (PCR) based analyses (Becker *et al.*, 1996; D'Amore *et al.*, 1997) and linear RNA amplification including amplified antisense RNA (aRNA) (Eberwine *et al.*, 1992, 2001; Ginsberg *et al.*, 1999a, 2000) and the newly developed terminal continuation (TC) RNA amplification (Che and Ginsberg, 2004, 2005; Ginsberg and Che, 2004; Ginsberg *et al.*, 2004) have been used in combination with single-cell microdissection procedures to enable the use of microarray analysis (Eberwine *et al.*, 2001; Ginsberg and Che, 2004). RNA amplification is a series of elaborate molecular-based methods used to amplify genomic signals in a linear fashion from minute quantities of starting materials for microarray analysis and other downstream genetic applications (Fig. 4.1). In this chapter, we illustrate the utility of combining discrete cell microdissection methodologies with RNA amplification for use in microarray analyses as well as pairing laser capture microdissection (LCM) with proteomic profiling for single cell and/or population cell resolution at the protein level. Utilization of tract-tracing methods in combination with gene expression analysis and proteomic profiling is also presented.

II. GENE EXPRESSION PROFILING USING FIXED TISSUES

A. Antemortem and Postmortem Variables

Assessment of single cell and homogeneous cell populations in optimally prepared, perfused fixed animal tissues as well as fixed postmortem human brain tissues is desirable due to the abundance of animal and human brain tissues that are archived within individual laboratories and brain banks and because of the use of relevant animal models to further understand disease mechanisms. At present, no consensus protocol exists for the fixation and/or extraction of brain tissues obtained from animals or from postmortem human tissues. Several laboratories have evaluated the effects of different fixation protocols on RNA quality, ease of tissue microdissection, and success of microarray analysis (Bahn *et al.*, 2001; Coombs *et al.*,

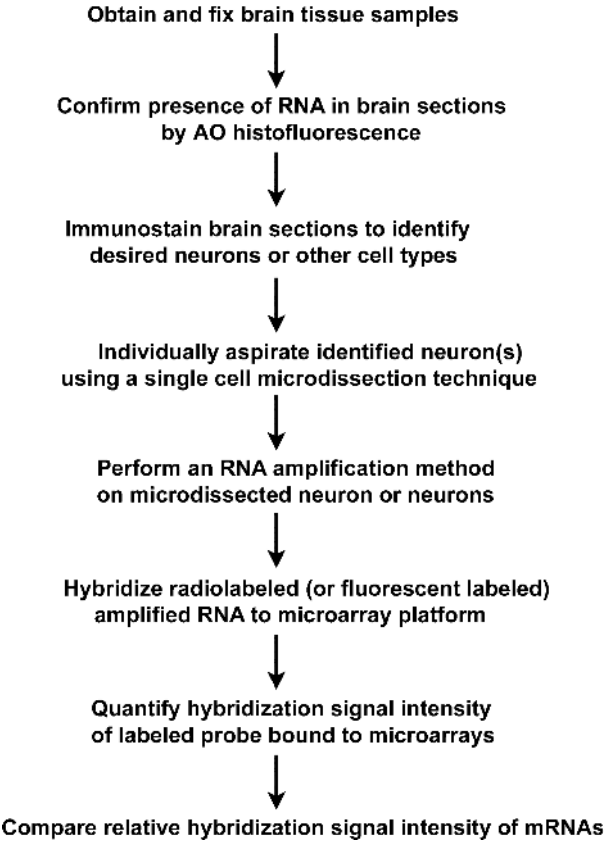

Figure 4.1. Schematic overview of the experimental design. Outline of the general procedures used to perform microdissection combined with high-throughput gene expression analysis using array platforms.

1999; Goldsworthy *et al.*, 1999; Van Deerlin *et al.*, 2000, 2002; Vincent *et al.*, 2002).

Despite potential advantages of discrete cell RNA amplification technology, several caveats must be considered when undertaking such studies in brain tissue. One factor is postmortem interval (PMI), or the time that elapses between time of death and preservation of the tissue sample. PMI is particularly relevant when obtaining postmortem human materials, as animal models can be fixed rapidly using perfusion techniques. Investigators must be cognizant of many factors including PMI and the time from dissection to tissue preservation that may affect the quality and quantity of recovered nucleic acids and proteins. Moreover, the choice of fixative for tissue preservation is an important factor affecting RNA stability. Fixatives include aldehydes (e.g., formalin, paraformaldehyde, and glutaraldehyde), alcohols (e.g., ethanol and methanol), oxidizing agents, and picrates. In general,

fixatives either create cross-links or exert a precipitative effect that may alter the native structure of macromolecules. With regards to neuroscience, aldehydes and alcohols are the most commonly used fixatives. Aldehydes induce cross-linkage of lysine residues formed in proteins, and alcohols are protein denaturants. The means by which RNA is preserved is unknown but likely involves the inactivation of degradative enzymes. The choice of fixative must be balanced between optimizing tissue morphology and preserving nucleic acid integrity for evaluation. As reviewed by Van Deerlin *et al.* (2000, 2002), ethanol and depolymerized 4% paraformaldehyde-based fixatives provide optimal results for molecular-based studies. Another factor is the agonal state of the human cases examined and the presence of overlapping neurologic conditions. Agonal state refers to the nature and time period between the onset of the terminal phase of an illness and death. The agonal state of a patient prior to death can have profound effects on several parameters including tissue pH, RNA stability, and protein degradation (Bahn *et al.*, 2001; Leonard *et al.*, 1993; Van Deerlin *et al.*, 2000, 2002). For example, hypoxia, pneumonia, and protracted coma have been associated with alterations in RNA and protein levels (Barton *et al.*, 1993; Hynd *et al.*, 2003; Tomita *et al.*, 2004). Therefore, numerous variables, including antemortem characteristics, agonal state, duration of fixation, and length of storage, are relevant parameters that should be considered prior to the initiation of molecular studies that utilized human postmortem tissues.

B. Acridine Orange Histofluorescence and Bioanalysis

Of critical importance in discrete cell RNA assessment, as well as other molecular procedures, is the evaluation of RNA quality and quantity. A useful and relatively quick method for assessing RNA quality in tissue sections prior to performing expression profiling studies is the use of acridine orange (AO) histofluorescence. AO is a fluorescent dye that intercalates selectively into nucleic acids (Mikel and Becker, 1991; von Bertalanffy and Bickis, 1956) and has been used to detect RNA and DNA in brain tissues (Ginsberg and Che, 2004; Topaloglu and Sarnat, 1989; Vincent *et al.*, 2002; Zoccarato *et al.*, 1999). Upon excitation in the ultraviolet spectra, AO that intercalates into RNA emits an orange-red fluorescence, whereas AO that intercalates into DNA emits a yellowish-green fluorescence. AO can also be combined with immunocytochemistry within tissue sections to double label cytoplasmic RNAs and specific antigens of interest, and is compatible with confocal microscopy (Ginsberg *et al.*, 1997). In brain tissue sections, the pale background of white matter tracts that lack abundant nucleic acids contrasts AO-positive neurons. Nonneuronal cells tend to have less AO histofluorescence as compared to neurons and brain tumor cells (Sarnat *et al.*, 1987), suggesting that there is less overall RNA. It is important to note that individual RNA species (e.g., rRNA, tRNA, and mRNA) cannot be delineated

by AO histofluorescence. Rather, this method provides a simple diagnostic test that can be performed on adjacent tissue sections to ensure the likelihood that an individual case has abundant RNA prior to performing expensive microdissection and microarray studies. A more definitive examination of RNA quality can be obtained via bioanalysis (e.g., 2100 Bioanalyzer, Agilent Technologies), which employs capillary gel electrophoretic methodologies to detect RNA quality and abundance (Che and Ginsberg, 2004, 2005; Ginsberg and Che, 2004). Bioanalysis enables visualization of results in an electropherogram and/or digital gel formats, and provides a means of RNA assessment at relatively high sensitivity. Investigators can also evaluate DNA and protein quality and abundance using bioanalysis platforms (Freeman and Hemby, 2004).

III. REGIONAL MICRODISSECTION METHODS

Microdissection of individual cells is performed to enable downstream gene expression profiling. Provided that procedures are performed on fresh, frozen, or well-fixed tissue sections and ribonuclease (RNase) free conditions are employed, both immunocytochemical and histochemical procedures can be utilized to identify specific cell(s) of interest (Ginsberg and Che, 2004, 2005). Several different methodologies have been used to aspirate individual cells or groups of cells including single-cell microaspiration and LCM techniques.

In addition to single-cell microdissection, regional dissections can also be performed, which may be useful to the investigator. Regional analysis is a powerful approach for the identification of transcripts that are enriched in a specific region, lamina, or nuclei that differ from adjacent or connected regions. Groups of related cells from discrete regions of brain or spinal cord can be readily dissected from paraffin-embedded tissue sections (e.g., 5–6 μm thick) or frozen tissue sections (e.g., 20–40 μm thick) by an experienced neuroanatomist. Unstained sections can be utilized, but optimal cellular resolution occurs using sections prepared for immunocytochemical or histochemical (e.g., Nissl stain) procedures. We have had success in scraping away areas of the tissue section that were not desired to reveal only the well-defined region of interest (Ginsberg and Che, 2002, 2004; Hemby *et al.*, 2002). Regional dissections can be performed on fresh, fixed, or thawed tissue blocks using a stereomicroscope along with a scalpel or micropunch. A caveat is that these approaches are highly operator dependent, and can be difficult to reproduce across samples. RNA is extracted from the resulting tissue for downstream applications, such as cDNA array analysis, quantitative real-time PCR (qPCR), serial analysis of gene expression (SAGE), and differential display, among others (Che and Ginsberg, 2005; Ginsberg and Che, 2002; Lein *et al.*, 2004; Zhao *et al.*, 2001). Regional dissections can also be used as the input source for protein in the case of fresh and/or frozen tissues for proteomics-based applications as well as for

conventional neurochemical and immunoblotting procedures (Freeman and Hemby, 2004; Mouledous *et al.*, 2003; Palkovits, 1989). An advantage of regional analyses is that limited RNA amplification is necessary to generate significant hybridization signal intensity. For example, microdissection of the basal forebrain, hippocampal formation, midbrain, and nucleus accumbens has been performed to generate regional expression profiles in normal brains and in pathological conditions including Alzheimer's disease (AD) and cocaine self-administration (Backes and Hemby, 2003; Fasulo and Hemby, 2003; Ginsberg and Che, 2002, 2004; Tang *et al.*, 2003). A disadvantage of regional dissection procedures is the lack of single-cell resolution, as neurons, nonneuronal cells, vascular elements, and epithelial cells will be included in the dissection.

IV. SINGLE-CELL MICROASPIRATION METHODS

Discrimination and isolation of adjacent cell types from one another is critical because this enables the selection of relatively pure populations of individual cells and/or populations for subsequent analysis and avoids potential contamination from a variety of sources including glia, vascular epithelia, and other nonneuronal cells within the brain. One method of isolating individual cells or populations of homogeneous cells is termed single-cell microaspiration. Single-cell microaspiration entails visualizing an individual cell (or cells) using an inverted microscope connected to a micromanipulator, microcontrolled vacuum source, and an imaging workstation on an air table. Electrophysiology rigs can also be modified to aspirate cells from fixed tissue sections with minor modifications. Handheld and syringe-pump-driven vacuum sources can also be utilized; however, they are difficult to control and may cause inadvertent damage to the tissue section. Individual cells are carefully aspirated from the tissue section of interest, and placed in microfuge tubes for subsequent RNA amplification (Fig. 4.2). This methodology results in accurate dissection of the neurons of interest with minimal disruption of the surrounding neuropil (Ginsberg, 2001; Ginsberg *et al.*, 2004; Hemby *et al.*, 2002; Mufson *et al.*, 2002). An advantage of utilizing a single-cell microaspiration technique is the extremely high cellular (and potentially subcellular, compartmental, and/or dendritic) level of resolution for aspiration of single elements (Crino *et al.*, 1998; Ginsberg and Che, 2005; Hemby *et al.*, 2003). Disadvantages include the relative difficulty of performing the aspirating technique, experimenter error, and the lengthy time allotment necessary to perform microaspiration, especially if multiple cells are being acquired from different brain tissue sections. Moreover, investigators should be aware of the degree of heterogeneity of the cells of interest and the extent to which small numbers of cells may or may not be representative of a population of interest.

A key aspect of the success of single-cell and single-population gene expression analysis is that different cell types can be discriminated based

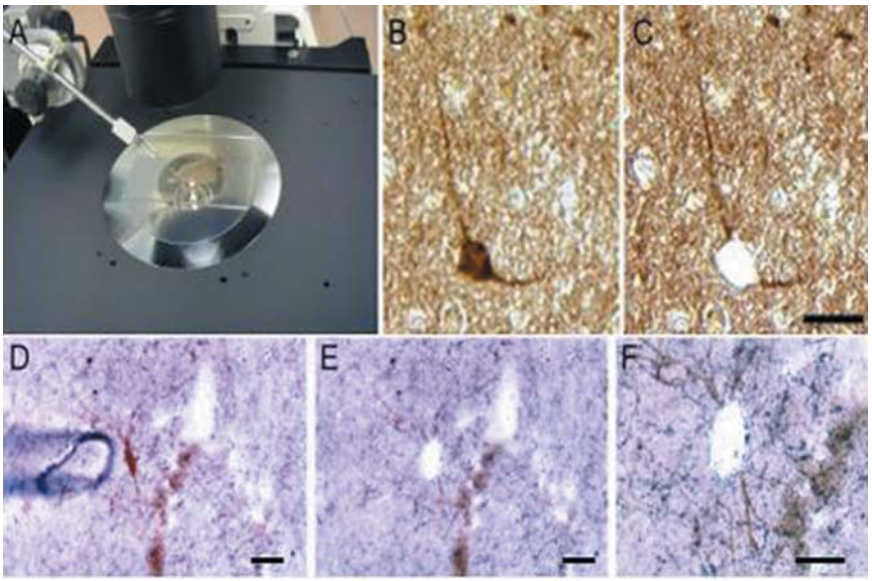

Figure 4.2. Microaspiration of single neurons. (A) Representative photomicrograph illustrating the placement of a human postmortem tissue section of the basal forebrain onto the microaspiration apparatus. (B) Section immunolabeled with an anti-neurofilament antibody depicting a representative layer II entorhinal cortex stellate cell obtained postmortem from a normal control human brain and the same section following microdissection of the immunostained neuron (C). Scale bar: 25 μm. (D) Human anterior nucleus basalis neuron visualized by dual immunolabeling for the cholinergic marker $p75^{NTR}$ (brown cell bodies) and galanin (black punctate fibers). The microaspirating pipette can be visualized in the left plane of the field shown in (D). Photographs of the same tissue section are shown following microaspiration of the cholinergic neuron at low (E) and higher magnification (F). Scale bars in (D)–(F): 40 μm.

on their molecular fingerprint. For example, populations of neurons that express proteins selectively such as cholinergic basal forebrain neurons (Mufson *et al.*, 2002, 2003) or midbrain dopaminergic neurons (Fasulo and Hemby, 2003; Tang *et al.*, 2003) are amenable to single-cell RNA amplification and subsequent cDNA array analysis. Cells that lack a distinct or selective phenotypic signature can be analyzed using a variety of Nissl and immunocytochemical stains for downstream genetic applications (Ginsberg and Che, 2004, 2005; Kamme *et al.*, 2003). Although histological stains are typically not specific to an individual cell type or protein, much information can be gleaned by utilizing classical histological preparations in conjunction with contemporary protein (e.g., immunocytochemistry) and molecular biological methodologies. For example, hematoxylin and eosin (H&E) staining has been performed in combination with microdissection and PCR-based strategies as well as microarray platforms using RNA amplification methods (Becker *et al.*, 1996; Goldsworthy *et al.*, 1999; To *et al.*, 1998). Moreover, we have demonstrated that several Nissl stains including cresyl violet, H&E, and thionin perform as well as immunocytochemistry in terms of hybridization

signal intensity detection when employing cDNA array analysis (Ginsberg and Che, 2004). In contrast, several dyes that bind to RNAs directly, such as AO and silver stain, do not perform well in combination with microdissection and subsequent cDNA array analysis (Ginsberg and Che, 2004).

V. LASER CAPTURE MICRODISSECTION

A. Introduction

The implementation of high-throughput microaspiration devices over the last few years has enabled rapid accession of single cells and homogeneous cellular populations for downstream genomic and proteomic analyses. Specifically, LCM is a strategy for acquiring histochemically and/or immunocytochemically labeled cells from in vivo and in vitro sources (Dolter and Braman, 2001; Ehrig *et al.*, 2001; Goldsworthy *et al.*, 1999; Lu *et al.*, 2004). LCM has become a widely used and reproducible technique that was developed originally at the NIH (Bonner *et al.*, 1997; Emmert-Buck *et al.*, 1996). There are two principal means of LCM: positive extraction and negative extraction.

B. Positive Extraction

Positive extraction (a method used by the PixCell IIe from Arcturus) employs a laser source directly on the cell(s) of interest for the purpose of microaspiration. There are four steps in positive extraction methods for capturing cells under direct visualization and recovering biomolecules. After locating the cells of interest in a tissue section, a small plastic cap (e.g., CapSure or CapSure HS LCM Cap) coated with a special thermoplastic film is placed over the area of tissue containing the cell targets. A nondestructive, low-power, near-infrared laser pulse is then directed through the cap at the target cell. The pulsed laser energy causes localized activation of the thermoplastic film that extends, embraces, and adheres to the target cell. Raising the thermoplastic cap separates targeted cells, now attached to the film, from surrounding undisturbed tissue (Fig. 4.3). Populations of cells attached to the cap are suitable for microscopic examination and downstream genetic analysis.

C. Negative Extraction

Negative extraction (or noncontact laser extraction) procedures employ a laser source to cut around the area of interest within a tissue section, and the microdissected material is catapulted into a microfuge tube (a method utilized by the PALM system, PALM Microlaser Technologies). A variety of conditions can modify the consistent success of cell capture, including tissue fixation. Tissues can be fresh, frozen, or fixed in alcohol or aldehydes

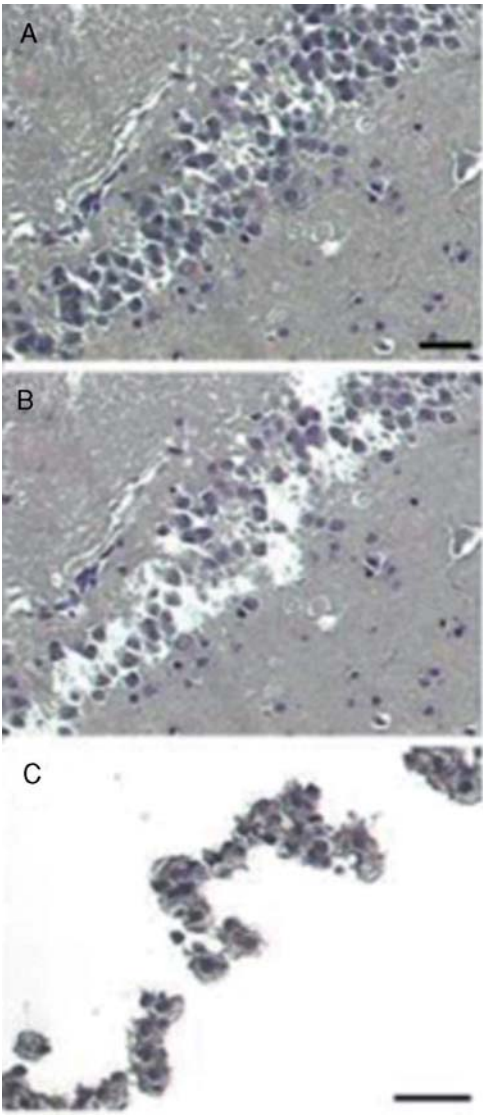

Figure 4.3. LCM of granule cells. Photomicrographs of a microaspiration of cresyl violet stained human hippocampal granule cells using LCM from a 6-μm thick ethanol fixed tissue section. (A) Section prior to LCM. (B) The cap is removed following laser pulses over desired cells, leaving spaces where microdissected granule cells originally resided. (C) Captured cells are visualized by placing the cap on a clean slide for contrast. Scale bar in (A) and (B): 25 μm; (C): 30 μm.

(Goldsworthy *et al.*, 1999; Su *et al.*, 2004). Other parameters include optimal section thickness (<10–14 μm) and the type of glass slide (e.g., uncoated, charged, poly-L-lysine, and gelatin-coated) used to mount the tissue sections for subsequent microdissection. Both positive and negative extraction

methods allow captured cells and their processes to be examined microscopically to confirm the identity and quality of isolated cell population(s). This quality control step ensures validity of the results obtained from downstream analysis. Single cells as well as dozens to hundreds of cells can be collected by LCM instrumentation. RNA, DNA, and protein can be extracted from microdissected cells and utilized as input sources for downstream applications such as microarray analysis, qPCR, as well as proteomics (Ehrig *et al.*, 2001; Fend *et al.*, 1999; Suarez-Quian *et al.*, 1999). We have utilized LCM to microdissect a variety of neuronal populations including hippocampal CA1 and CA3 neurons, dentate gyrus granule cells, and spinal motor neurons (see below) from mouse brains and postmortem human brains (Che and Ginsberg, 2004, 2005; Ginsberg and Che, 2002, 2004, 2005). LCM has been increasingly utilized to collect cells for downstream proteomic analyses including two-dimensional gel electrophoresis, tandem mass spectroscopy, and antibody-based protein chips (Craven *et al.*, 2002; Freeman and Hemby, 2004; Mouledous *et al.*, 2003; Simone *et al.*, 2000). In summary, the ability to access DNA, RNA, and protein from microdissected tissue samples via LCM-based technologies represents an exciting new avenue for studying homogeneous populations of brain cells.

VI. TRACT-TRACING COMBINED WITH DISCRETE CELL MICRODISSECTION

The combination of discrete cell dissection and RNA amplification allows the investigator to make specific assertions about disease- or drug-induced changes in gene and protein expression with unique certainty. Tract-tracing methodologies extend this capability by providing the means to identify and isolate specific processes and/or pathways of interest based on connectivity. Various tracers are employed to label neurons and neuronal processes in anterograde, retrograde, and bidirectional vectors. A discourse on the advantages and disadvantages of individual tracers is beyond the scope of this chapter. However, selection criteria depend on the experimental paradigm and the cell, region, or tissue type of interest (see these chapters in the current book for additional detail) (Lanciego and Wouterlood, 2006; Molnar *et al.*, 2006; Reiner and Honig, 2006).

Hemby and colleagues have undertaken a series of studies to evaluate the effects of psychotropic compounds on midbrain dopaminergic neurons as defined by their axonal targets (Backes and Hemby, 2003; Fasulo and Hemby, 2003). For example, in order to explore gene expression changes in tegmental-accumbal dopamine neurons following cocaine administration, the retrograde tracer Fluorogold (FG) was iontophoretically injected into the nucleus accumbens of rats. Following a 2-week period to allow for sufficient transport of the tracer, rats were sacrificed and the localization of injections was assessed by fluorescence microscopy. As depicted in Fig. 4.4A, a number of ventral midbrain neurons in the area corresponding

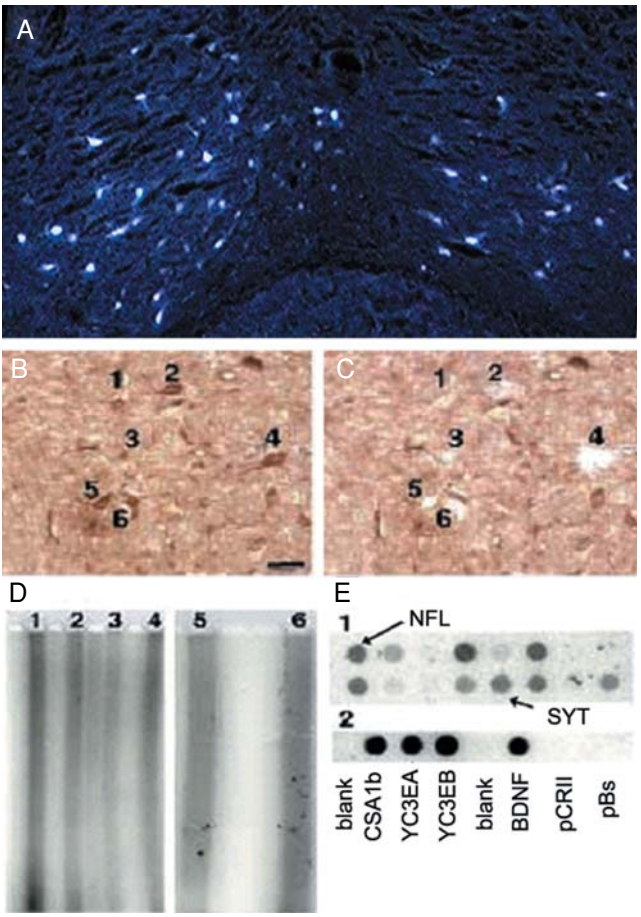

Figure 4.4. Tract-tracing in combination with microdissection and array analysis. (A) Representative section from rat midbrain for identification of FG-labeled cells. FG (4%) was iontophoresed into the nucleus accumbens of rats 2 weeks prior to sacrifice. Photomicrograph reveals significant midbrain FG-labeling within the ventral tegmental area of Tsai. (B) A representative section within the midbrain is shown following immunocytochemistry using an anti-FG antibody suitable for microaspiration. Scale bar: 20 μm. (C) FG-immunoreactive individual neurons were microdissected from the tissue section. (D) The six cells in B (1–6) were amplified by two rounds of aRNA and labeled with ^{32}P-CTP. aRNA was run on a 1% denaturing gel [numbers above each lane correspond to neurons in (B) and (C)]. (E) Radiolabeled aRNA from neuron #2 was used as a probe for identifying candidate cDNAs on a custom-designed array (E1) and subcloned differential display products (E2). Key (E1) top row; neurofilament-L (arrow); casein kinase II b; H67559; AA069725; T89891; AA076650; pulmonary surfactant associate protein (control); heme oxygenase 1 (control): bottom row; CG1 protein precursor; H89874; H70730; H89236; syntaxin (SYT; arrow); T92612; T90579; stathmin. Key (E2): blank; CSA1b; YC3EA; YC3EB; blank; brain derived neurotrophic factor (BDNF); vector (pCR II); vector (pBS). Accession numbers correspond to individual expressed sequence-tagged cDNAs (ESTs).

to the ventral tegmental area were FG-positive. Since not all of the projecting cells of the ventral midbrain are dopaminergic, the midbrain sections processed for tyrosine hydroxylase immunofluorescence to ensure assessment of dopamine-containing neurons using a mouse anti-tyrosine hydroxylase visualized with a Cy5 conjugated donkey anti-mouse secondary antibody. The procedure of dual labeling provides both certainty of anatomical connectivity and antigen specificity of the cells of interest. Alternatively, if cell-specific antigens are not available, antibodies directed against FG can be used to identify labeled neurons for microdissection and subsequent downstream genetic analyses (Fig. 4.4). When using a nonspecific antigen or histochemical stain to identify labeled neurons, it is imperative to further characterize the cell type post hoc using a validation technique such as qPCR. Multiple tracers can also be used within the same subject to identify different cell populations based on connectivity. Utility of employing multiple fluorescent tracers is dependent on the absorption/emission spectra. For example, we have used up to four tracers in rhesus monkeys to identify different populations of midbrain dopaminergic cells based on different projection paths (i.e., dorsolateral prefrontal cortex, orbitofrontal cortex, nucleus accumbens, and caudate/putamen) (Freeman and Hemby, 2004).

Investigators must be cognizant of various caveats when using tract-tracing methodologies. For example, the use of iontophoretic injections limits neuronal damage and the potential interpretational confound of labeling fibers en passant. The ability to iontophorese tracers may be limited by the chemical nature of the tracer and/or the vehicle required to solubilize the tracer. In addition, the influence of tracer uptake on neuronal function remains a relevant question. To date, equivocal data imply that tracers may damage RNA and/or protein integrity of cells in which the tracer is sequestered (Emsley *et al.*, 2001; Franklin and Druhan, 2000). Therefore, additional dose-response and toxicity studies are warranted to examine the extent to which various tracers may influence RNA and protein expression in neuronal populations.

VII. RNA AMPLIFICATION

A. aRNA

In order to generate a significant amount of RNA sufficient to perform microarray analysis and related high-throughput genetic readouts, an RNA amplification technique is often required when attempting expression profiling from single neurons, groups of neurons, or microdissected regions. PCR-based amplification methods are not optimal, as exponential amplification can skew the original quantitative relationships between genes from an initial population (Kacharmina *et al.*, 1999). Linear RNA amplification is another strategy that has been used successfully to generate enough input RNA for robust hybridization signal intensity on array platforms. The

initial method of linear amplification termed aRNA amplification was developed by Eberwine and colleagues, and involves a T7 RNA polymerase-based amplification procedure that enables quantitation of the relative abundance of gene expression levels from identified single cells and populations (Eberwine *et al.*, 1992, 2001; Kacharmina *et al.*, 1999; Phillips and Eberwine, 1996). The resultant amplified aRNA maintains a proportional representation of the size and complexity of the initial input mRNAs (Eberwine *et al.*, 1992; VanGelder *et al.*, 1990). aRNA amplification entails the hybridization of a 66 basepair oligonucleotide primer consisting of 24 thymidine triphosphates (TTPs) and a T7 RNA polymerase promoter sequence [oligo d(T)T7] to mRNAs and conversion to an mRNA–cDNA hybrid by reverse transcriptase (Tecott *et al.*, 1988; VanGelder *et al.*, 1990) (Fig. 4.5). Upon conversion of the mRNA–cDNA hybrid to double-stranded cDNA, a functional

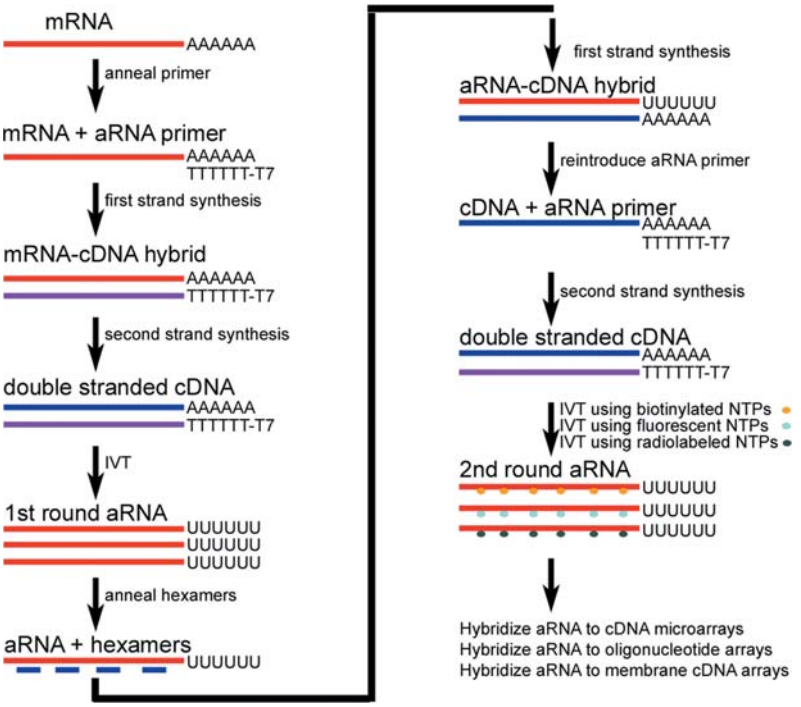

Figure 4.5. aRNA amplification scheme. An oligo d(T)T7 primer is hybridized to polyA+ mRNAs and a double-stranded mRNA–cDNA hybrid is formed by reverse transcription. The double-stranded mRNA-cDNA hybrid is then converted into double-stranded cDNA. Following the removal of tertiary structures and drop dialyzing the double-stranded cDNA against RNase-free water, the first round of aRNA synthesis occurs via in vitro transcription (IVT) using T7 RNA polymerase and NTPs. The second round of aRNA amplification begins by annealing random hexamers to the newly formed aRNA, and synthesizing a cDNA strand. The oligo (dT)T7 primer is then reintroduced and a double-stranded cDNA template is formed. aRNA probes are then generated with fluorescent, biotin, or radiolabeled second-round aRNA products.

T7 RNA polymerase promoter is formed. aRNA synthesis occurs with the addition of T7 RNA polymerase and nucleotide triphosphates (NTPs). Each round of aRNA results in an approximate 1000-fold amplification from the original amount of each polyadenylated [poly(A)+] mRNA in the sample (Eberwine *et al.*, 1992, 2001). Two rounds of aRNA are typically necessary to generate sufficient quantities of aRNA for subsequent downstream analyses. aRNA products are biased toward the 3′ end of the transcript due to the priming at the poly(A)+ RNA tail (Kacharmina *et al.*, 1999; Phillips and Eberwine, 1996). This 3′ bias exists for all amplified aRNA products and relative levels of gene expression can be compared (Che and Ginsberg, 2004; Madison and Robinson, 1998; Phillips and Eberwine, 1996). Moreover, amplified aRNA products tend not to be of full length (Ginsberg *et al.*, 1999a; Kacharmina *et al.*, 1999; Phillips and Eberwine, 1996). Although aRNA is a laborious and difficult procedure, we have generated successful results obtained from microaspirated cells from animal model and postmortem human brain tissues utilizing a wide variety of array platforms (Ginsberg *et al.*, 1999a, 2000; Hemby *et al.*, 2002, 2003; McClain *et al.*, 2005).

Several different strategies have been employed by independent laboratories to evaluate and improve linear RNA amplification efficiency (Iscove *et al.*, 2002; Klur *et al.*, 2004; Matz *et al.*, 1999; Wang *et al.*, 2000). The principal obstacle is the problematic second strand cDNA synthesis. This impediment is not specific to the aRNA protocol. Rather, this issue is endemic to all current RNA amplification methods. Key factors to improving RNA amplification include increasing the efficiency of second-strand cDNA synthesis and allowing for flexibility in the placement of bacteriophage transcriptional promoter sequences.

B. TC RNA Amplification

We have developed a new linear RNA amplification procedure that utilizes a method of terminal continuation. TC RNA essentially consists of synthesizing first-strand cDNA complementary to the RNA template, subsequently generating second-strand cDNA complementary to the first-strand cDNA, and finally IVT using the double-stranded cDNA as template (Che and Ginsberg, 2004, 2005) (Fig. 4.6). Synthesis of the first-strand cDNA complementary to template mRNA entails the use of two oligonucleotide primers: a poly d(T) primer and a TC primer. The poly d(T) primer is similar to conventional primers that exploit the poly(A)+ sequence present on most mRNAs. The TC primer consists of an oligonucleotide sequence at the 5′ terminus and a short span of three cytidine triphosphates (CTPs) or guanosine triphosphates (GTPs) at the 3′ terminus. In this manner, single-strand cDNA synthesis can be initiated by annealing a second oligonucleotide primer complementary to the attached oligonucleotide (Che and Ginsberg, 2004). By providing a known sequence at the 3′ region of first-strand cDNA and a primer complementary to it, hairpin loops will not form. Second-strand

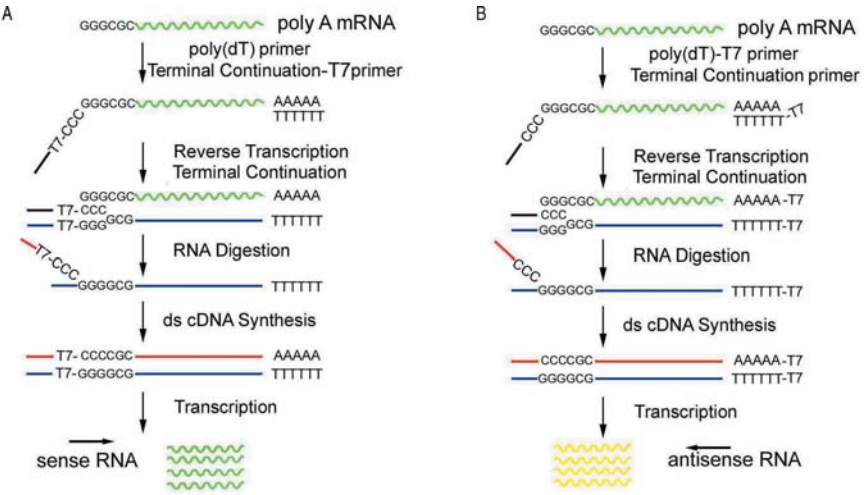

Figure 4.6. Overview of the TC RNA amplification method. (A) A TC primer (containing a bacteriophage promoter sequence for sense orientation) and a poly d(T) primer are added to the mRNA population to be amplified (green rippled line). First-strand (blue line) synthesis occurs as an mRNA–cDNA hybrid and is formed after reverse transcription and terminal continuation of the oligonucleotide primers. Following RNase H digestion to remove the original mRNA template strand, second-strand (red line) synthesis is performed using *Taq* polymerase. The resultant double-stranded product is utilized as template for IVT, yielding high-fidelity, linear RNA amplification of sense orientation (green rippled lines). (B) Schematic similar to (A), illustrating the TC RNA amplification procedure amplifying RNA in the antisense orientation (yellow rippled lines).

cDNA synthesis can be performed with robust DNA polymerases, such as *Taq*, and the TC reaction is highly efficient. One round of amplification is sufficient for downstream genetic analyses (Che and Ginsberg, 2004; Ginsberg and Che, 2004). Furthermore, TC RNA transcription can be driven using a promoter sequence attached to either the 3′ or the 5′ oligonucleotide primers. Therefore, transcript orientation can be in an antisense orientation (similar to conventional aRNA methods) when the bacteriophage promoter sequence is placed on the poly d(T) primer or in a sense orientation when the promoter sequence is attached to the TC primer, depending upon the design of the experimental paradigm (Fig. 4.6). TC RNA amplification offers high sensitivity, flexibility, and throughput capabilities for downstream genetic analyses. Following TC RNA amplification, a large proportion of genes can be assessed quantitatively as evidenced by bioanalysis and cDNA microarray analysis in mouse and human postmortem brain tissues (Che and Ginsberg, 2004; Ginsberg and Che, 2002, 2004, 2005; Mufson *et al.*, 2002). Robust linear amplification is consistently observed. Amplification efficiency of approximately 2500- to 3000-fold is demonstrated with commercially available purified mRNAs, and approximately 1000- to 1500-fold amplification is found after one round using biological samples of RNA

extracted from a variety of brain sources (Che and Ginsberg, 2004). Results indicate a high degree of expression level similarity for high, moderate, and low expressed genes using the TC RNA amplification method. The threshold of detection of genes with low hybridization signal intensity is also greatly increased, as many genes that are at the limit of detection using conventional aRNA can be readily observed with the TC method (Che and Ginsberg, 2004). Importantly, increased sensitivity appears greatest for genes with relatively low abundance. Moreover, background hybridization is significantly attenuated when using TC RNA amplification (Ginsberg and Che, 2002, 2004; Mufson *et al.*, 2002).

VIII. MICROARRAY ANALYSIS OF MICRODISSECTED SAMPLES

Once an RNA amplification procedure is utilized to increase the input source of RNA species, biotinylated, fluorescent, or radiolabeled probes can be generated for subsequent hybridization to microarray platforms. Technical advances have fostered the development of high-density microarrays that allow for high-throughput analysis of hundreds to thousands of genes simultaneously. Synthesis of cDNA microarrays entails adhering cDNAs or ESTs to solid supports such as glass slides, plastic slides, or nylon membranes (Brown and Botstein, 1999; Eisen and Brown, 1999). A parallel technology uses photolithography to adhere oligonucleotides to array media (Lockhart *et al.*, 1996). Gene expression is assayed by harvesting total RNA or mRNA from sample tissues, labeling either by radioactive or by fluorescent methods, and hybridizing the labeled probes to arrays (Fig. 4.7). Arrays are washed to remove nonspecific background hybridization, and imaged using a laser scanner for biotinylated/fluorescently labeled probes and a phosphor imager for radioactively labeled probes. The specific signal intensity (minus background) of amplified RNA bound to each probe set (e.g., oligonucleotides or cDNAs/ESTs) is expressed as a ratio of the total hybridization signal intensity of the array, thereby minimizing variations due to differences in the specific activity of the probe and the absolute quantity of probe present. Gene expression data collected using single cells and/or homogeneous populations via RNA amplification and microarray analysis do not allow absolute quantitation of mRNA levels, but generate an expression profile of the relative changes in mRNA levels (Eberwine *et al.*, 2001; Galvin and Ginsberg, 2004; Ginsberg and Che, 2002; Ginsberg *et al.*, 2004; Hemby *et al.*, 2003; Madison and Robinson, 1998; Mufson *et al.*, 2002). Relative changes in individual mRNAs are analyzed by univariate statistics [e.g., analysis of variance (ANOVA) with post hoc Neumann–Keuls test] for individual comparisons (Ginsberg *et al.*, 1999a, 2000; Hemby *et al.*, 2002; Mufson *et al.*, 2002). Differential expression greater than approximately twofold is accepted conventionally as relevant for further examination (Freeman and Hemby, 2004; Galvin and Ginsberg, 2004; Ginsberg *et al.*, 2004; Hemby *et al.*, 2003; Mirnics *et al.*, 2000). Differentially expressed genes can be clustered

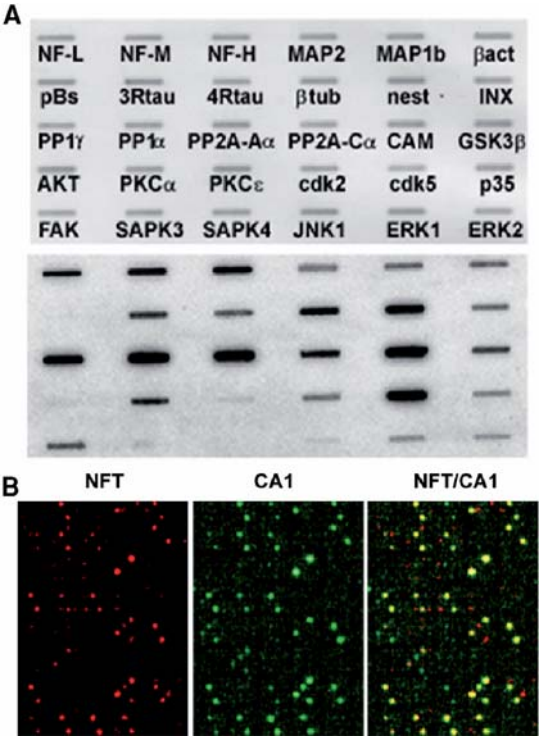

Figure 4.7. Representative array platforms. (A) A custom-designed cDNA array with 30 lanes is depicted. cDNAs are stained with bromophenol blue to show equal loading (top panel). The same array (A; bottom panel) is shown following hybridization with radiolabeled aRNA from a single CA1 neuron. Note the differential expression and abundance of cDNAs. (B) A portion of a high-density cDNA microarray, illustrating aRNA probes generated from neurofibrillary tangle (NFT)-bearing neurons (first panel; red), normal CA1 neurons (second panel; green), and an overlay of both (third panel). Yellow shows similar intensities for NFTs and normal neurons, green indicates a down regulation in NFTs relative to normal CA1 neurons, and red denotes an up regulation.

into functional protein categories for multivariate coordinate gene expression analyses (Freeman and Hemby, 2004; Ginsberg and Che, 2002; Kotlyar *et al.*, 2002). Computational analysis is critical for optimal use of microarrays due to the enormous volume of data that is generated from a single probe. Additionally, access to relational databases is desirable, especially when evaluating hundreds of ESTs that may or may not be linked to genes (and subsequent proteins) of known function.

IX. LCM IN COMBINATION WITH PROTEOMIC APPLICATIONS

Genomic and proteomic expression studies of tissues can be confounded easily because the cells of interest, for example, neurons, exist within a

heterogeneous environment that contains many types of cells. LCM allows the isolation of neurons on a single-cell basis for cell-specific analysis (see section "Laser Capture Microdissection"). Once captured, these relatively pure cell populations can be analyzed using a variety of methods, including downstream proteomic applications. Specifically, intact proteins and mRNA can be recovered from LCM captured cells and analyzed quantitatively. For protein studies, the surface-enhanced laser desorption/ionization time-of-flight mass spectrometry (SELDI-TOF MS) approach is an excellent way to evaluate neuron proteomics using the ProteinChip Biology System (PBSII, Ciphergen Biosystems) (Issaq *et al.*, 2002). The PBSII uses SELDI-TOF MS to retain proteins on a solid-phase chromatographic surface that are subsequently ionized and detected by TOF MS. Protein profiles can be generated from as few as 25–50 cells (Paweletz *et al.*, 2001). The SELDI-TOF MS technology consists of three major components: the ProteinChip array, the chip reader apparatus, and the software. The ProteinChip array is a 10-mm-wide × 80-mm-long platform having 8 (or 16) 2-mm spots comprising a specific chromatographic surface. Each spot contains either a chemically (e.g., anionic, cationic, hydrophobic, and hydrophilic) or biochemically (e.g., antibody and receptor) treated surface for retaining entire classes of proteins or single target proteins, respectively. Chemically treated surfaces retain whole classes of proteins, while surfaces treated with biochemical agent (e.g., antibody or other type of affinity reagent) serve as bait and will interact with a specific target protein. Biochemically treated arrays are custom-made by the user. Sample (1–10 μl of protein extract from captured neurons) is applied to the surface, with protein specificity being achieved via the surface treatment and the application of solvents/buffers and washes. After an energy-absorbing molecule solution is added, the array is inserted into the ProteinChip reader to measure the molecular weight and relative amounts of bound proteins. The reader is a laser desorption ionization mass spectroscopy instrument equipped with a pulsed ultraviolet nitrogen laser. Laser activation of the sample causes its desorption/ionization and liberation of gaseous ions from the ProteinChip arrays. The ions enter the TOF MS module that measures the mass-to-charge ratio of each protein. Protein detection is displayed as a series of peaks. The readout generated by the TOF MS analysis is a trace showing the relative abundance versus the molecular weights of the detected proteins. The software converts the peak trace into a simulated one-dimensional gel electrophoresis display to identify differences in protein abundances between samples. This technology can be used to determine in normal and degenerating neurons at specific structural stages patterns of protein expression and the levels of specific proteins and specific posttranslationally modified proteins (e.g., cleaved, phosphorylated, and acetylated proteins).

A practical example illustrating the union of LCM and proteomics using postmortem human spinal cord is provided in Fig. 4.8. LCM can be used to isolate individual spinal motor neurons, yielding a pure cell preparation for downstream proteomic applications (Fig. 4.8A,B). Motor neurons are

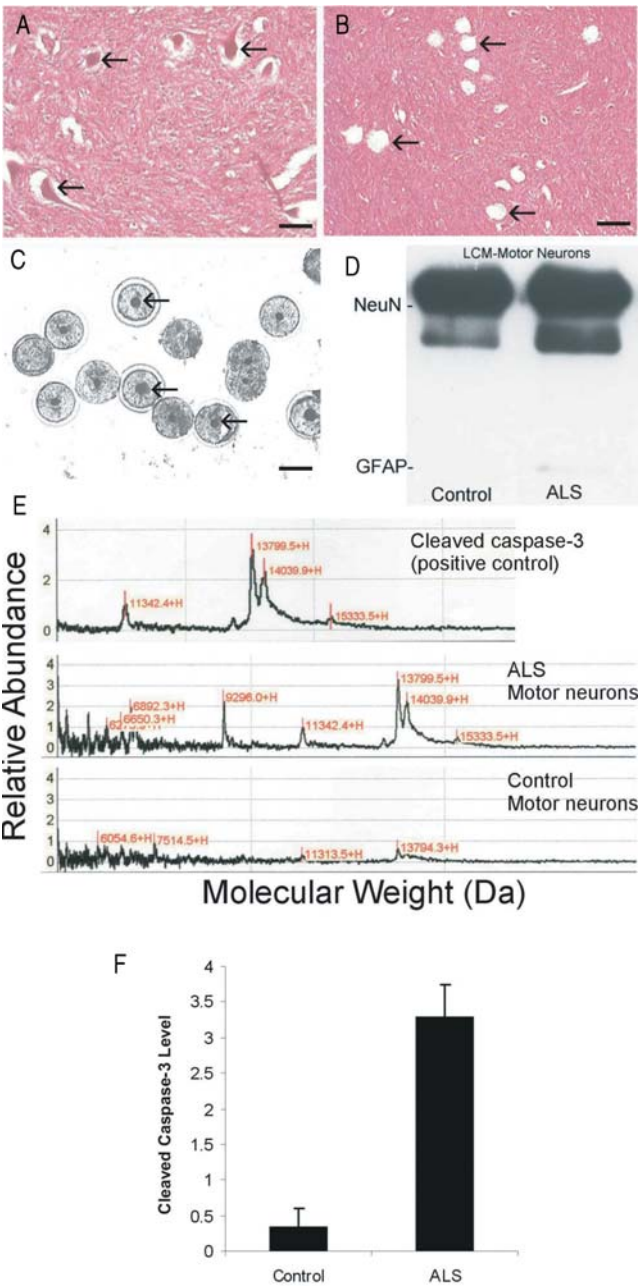

Figure 4.8. LCM and SELDI-TOF MS analysis of human ALS motor neurons. (A) Visualization of spinal cord motor neurons (arrows) in a Ponceau S stained cryostat section of human lumbar cord. Scale bar: 75 μm. (B) Human spinal cord section after harvesting motor neurons via LCM. The open empty circles in the section (arrows) show where the motor neurons were formerly located. Scale bar: 100 μm. (C) Confirmation of cell capture by direct visualization of caps with isolated motor

ideal for LCM because they are relatively large neurons with a low packing density. For example, we have used Ponceau S stained tissue sections to isolate target motor neurons from the surrounding neuropil for SELDI-TOF analysis. Captured cells can be viewed microscopically for confirmation (Fig. 4.8C). Moreover, Western blotting can be used to characterize the purity of human LCM samples. Astrocyte contamination, as assessed by glial fibrillary acidic protein (GFAP), is negligible. A high level of the neuronal nuclear protein NeuN and a very low level of GFAP in motor neuron cell lysates confirm the neuronal purity of the LCM samples (Fig. 4.8D). Even with long exposure times GFAP levels are barely detectable in motor neuron samples. Conversely, when cells with an astrocyte morphology are captured, the GFAP level is high and NeuN was not detectable. These pure motor neuron and astrocyte populations can be used for precise downstream molecular analysis of cell-specific events.

An example of the high resolution afforded by these types of applications is that the cell death protein, cleaved caspase-3, can be measured directly in human motor neurons obtained postmortem from normal control brains and subjects with amyotrophic lateral sclerosis (ALS). Approximately 14,000–15,000 motor neurons were isolated from fresh cryostat sections (stained with Ponceau S) from control lumbar spinal cords (three different cases for a total of ~45,000 motor neurons) and approximately 8000–10,000 motor neurons from ALS spinal cords (three different cases for a total of ~30,000 motor neurons) that were in the somatodendritic attritional stage of degeneration (Martin, 1999). Cleaved caspase-3 antibody (Cell Signaling Technology) was covalently bound to the surface of preactivated ProteinChip arrays (PS2 arrays, affinity capture surfaces). Covalently bound

←

Figure 4.8. (*Cont.*) neurons. The harvested motor neurons are surrounded by thermoplastic film. Scale bar: 225 μm. (D) Assessment of the purity of cell isolation by Western blotting of lysates of LCM acquired cells for NeuN and GFAP. Astrocyte contamination, as assessed by GFAP, is negligible. The high level of NeuN and very low level of GFAP in motor neuron cell lysates confirm the neuronal purity of the LCM samples. Even with long exposure times GFAP levels were only barely detectable in motor neuron samples from ALS cases. (E) Protein profiling in human ALS and control motor neurons by SELDI-TOF MS. PS2 ProteinChip arrays were used to isolate and quantify cleaved caspase-3. After sample preparation, the ProteinChip arrays were analyzed by laser desorption ionization TOF MS. For comparison purposes, the software of the SELDI Ciphergen system displays the data as a spectra view. Recombinant cleaved caspase-3 served as a positive control for identifying the molecular weights of the cleaved subunits. (F) Quantification of cleaved caspase-3 in human motor neurons. To identify differences in protein abundances between control and ALS cases, the software converts the peak trace into a simulated one-dimensional gel electrophoresis display to measure protein abundance. The values are mean ± standard deviation (SD). The measurements are normalized to parallel analyses of NeuN levels in the lysates. ALS motor neurons have significantly elevated ($p < 0.001$) levels of cleaved caspase-3 compared to age-matched controls (ANOVA with post hoc Neumann–Keuls test).

immunoglobulin (IgG) served as an antibody negative control. Crude cell lysates of captured motor neurons were applied to the ProteinChip with bound antibody, incubated, washed, and analyzed in a Ciphergen ProteinChip reader. Purified recombinant active caspase-3 (Medical and Biological Laboratories) was used as a positive control (Fig. 4.8E, upper retentate map) and it displayed prominent peaks at ~11.3, 13.8, and 14 kDa. Peptides corresponding to cleaved caspase-3 were found in ALS motor neurons (Fig. 4.8E, middle retentate map, peaks at ~11 and 14 kDa). No caspase-3 signal was observed in ALS or control cases with the nonspecific IgG bound to the chip. In age and postmortem delayed-matched control motor neurons, peaks of similar molecular weight were either not above background or were low (Fig. 4.8E, control motor neurons, lower retentate map). Quantification of cleaved caspase-3 (13.8 kDa protein) levels in control and ALS spinal motor neurons revealed highly significant ($p < 0.001$) increases in ALS motor neurons (Fig. 4.8F). The immunoassay results had remarkably low variability, likely due in part to the homogeneous population of motor neurons that was accrued via LCM.

Cell-based assays are critical for evaluating changes in protein cells undergoing degeneration. The use of tissue homogenate-based assays is suboptimal for this purpose because tissue homogenates cannot afford sufficient resolution. Thus, the interpretation of homogenate-based assays of tissues with a heterogeneous cellular composition is suspect. The strategy for measuring proteins in cells acquired via LCM represents a major step forward in the analysis of cell-specific degenerative events (Freeman and Hemby, 2004; Mouledous *et al.*, 2003). LCM and proteomic approaches are feasible and practical to apply, providing the availability of the equipment and service maintenance. The cellular resolution attained by LCM-based technologies for downstream proteomic applications is optimal for these types of in vivo investigations. LCM dramatically decreases the noise in the assays by minimizing contaminating cells. The integrity of the proteins and peptide fragments to be analyzed is maintained (Freeman and Hemby, 2004; Mouledous *et al.*, 2003). A pitfall of LCM-based technologies is that they are labor-intensive, and the number of captured cells required for quantitative signal detection is significant. However, the data gleaned by these types of studies represent definitive cell-specific events.

In summary, the analysis of human material as well as of appropriate animal models of neurodegeneration will provide direct results on the molecular events occurring within diseased cells. Employing LCM in combination with SELDI-TOF is ideal for dealing with asynchrony of neurodegeneration by providing structural–molecular correlations on neurons sampled at similar (and different) stages of degeneration. Human tissue experiments must be controlled at several levels with disease-specific controls that are matched for age, agonal state, and postmortem delay (Bahn *et al.*, 2001; Hynd *et al.*, 2003; Van Deerlin *et al.*, 2000, 2002). Moreover, interregional controls within the same case are necessary to rule out the possibility that observed changes are due to agonal state and tissue autolysis. Parallel studies of neurodegeneration in optimally prepared animal models can provide

valuable side-by-side comparisons of relevant molecules. Thus, molecular profiles can be then brought into the context of the structural phenotype of the observed degeneration. Moreover, if captured cells (using regional, microaspiration, and/or LCM-based technologies) obtained from an animal model display expression profile(s) that differ vastly from the human condition it is designed to model, applicability comes into question. Ultimately, a particular animal model may be deemed to be inappropriate for further study within the context of single cell or homogeneous population cell analysis based on disparities in genomic and proteomic profiles from a human condition that they were designed to mimic.

X. ADVANTAGES/LIMITATIONS

A variety of tissues and cells can be used to extract mRNA for gene profiling experiments. When employing mRNA as a starting material, one cannot overemphasize the importance of the preservation of RNA integrity. RNA species are particularly sensitive to degradation by RNase. RNases are found in virtually every cell type, and they retain their activity over a broad pH range (Blumberg, 1987; Farrell, 1998). Thus, RNase-free precautions are essential for all microdissection-based studies. All biological samples require prompt handling, either through rapid RNA extraction, flash freezing, or through fixation to minimize degradation.

Reproducibility of single-cell expression profiling is a critical parameter that is improving. Advances at the level of tissue dissection, RNA amplification, microarray platforms, and developing powerful statistical methods will ultimately lead to greater utility and flexibility of these technologies. Recent advances include the utilization of pooled populations of individual cell types to reduce variability in expression levels yet maintain an expression profile for a single cell type. The likelihood of generating highly reproducible data is increased greatly by replicate array analysis of aliquots of the same amplified RNA sample. Validation of array results is important, and several independent alternative techniques are quite useful to reproduce changes seen on an array platform such as qPCR, SAGE, and/or in situ hybridization, among others.

When deciding whether or not to employ microaspiration and/or high-throughput array technologies, the most important aspect to consider is the question the researcher is interested in answering, and determining the method(s) that would be best suited to perform the experiment. Once a researcher has decided that an array experiment is appropriate, much consideration needs to go into sample size and preparation, tissue and/or cell quality, and importantly, input amount of RNA that will likely be generated. If the input source is a small sample of population of cells captured by LCM, then an RNA amplification method is requisite. A researcher then needs to calculate laboratory and technical effort, cost, and goals in order to determine the commitment level that will be needed to carry out array experiments. Sample preparation, RNA amplification, array hybridization,

and array analysis usually require a long-term commitment, as many investigators have found out much to their dismay. A qPCR experiment would be more useful, for instance, if a researcher is trying to assess the regulation of a single gene product (or splice variants/isoforms of an individual gene family). An array experiment may yield the desired result, along with a plethora of potential data on dozens, hundreds, thousands of genes that may not be germane to central hypothesis. Quantitation of array platforms is typically relative, whereas qPCR can be more direct, using cycle threshold calculations as well as copy number (but this is difficult and not typically feasible for the casual qPCR user). qPCR can be reliable and cost effective, provided that the primer design is performed optimally. Alternatively, the solution hybridization afforded by RNase protection assays cannot be underestimated. RNase protection assays are especially useful when input sources of RNA are abundant, such as with in vitro paradigms. However, RNase protection assays in tissue sections, particularly fixed tissues, are not highly recommended. In summary, cDNA and oligonucleotide arrays are spectacular tools for high-throughput analyses within a myriad of paradigms and tissue sources. qPCR is a useful medium to low-throughput method that directly assays genes of specific interest. Our laboratory strategy is to combine the use of both assays, by defining expression profiling patterns on microarray platforms and validating individual gene level changes by independent qPCR analyses (Ginsberg and Che, 2004, 2005; Ginsberg *et al.*, 2004).

The combination of discrete cell microdissection procedures with microarray technologies allows for high-resolution, high-throughput expression profiling of dozens to hundreds to thousands of genes and proteins simultaneously from a single neuron or from a group of similar neurons. The next level of understanding of cellular and molecular mechanisms underlying normative function and pathological conditions lies in the ability to combine these aforementioned technologies with appropriate models to recapitulate the structure and connectivity of these systems in vivo and in vitro. Complex biological processes are not likely to be governed solely by the action of a single isolated gene. Rather, coordinate interactions of a multiplicity of genes may regulate normative function. When these gene programs or mosaics undergo increased or decreased expression during the lifespan, they may contribute to the mechanisms underlying disease pathogenesis. Single-cell and population-cell profiling techniques coupled with microarray platforms have the potential to quantify simultaneous expression levels of numerous genes and proteins in a given cell, thereby allowing for previously unobserved gene interactions, and ultimately protein interactions, to become more evident. Independent verification of individual gene level changes discovered by microarray analysis by alternate techniques is a critical component to a research program. Thus, a combination of multidisciplinary approaches is ideal for verification of gene expression level alterations, with the explicit knowledge that the sum of the evaluations may be more informative and reflect the actual biology of the system than an individual method.

APPENDIX: DETAILED METHODOLOGY

A. Acridine Orange Histofluorescence

This protocol was developed for AO histochemistry using animal model and human postmortem tissues embedded in paraffin (Ginsberg *et al.*, 1997, 1998; Mikel and Becker, 1991). Briefly, tissue sections are deparaffinized in xylene, graded through a descending ethanol series, and placed in distilled water for 5 min. The sections are placed in a 0.2 M dibasic sodium phosphate/0.1 M citric acid (SC; pH 4.0) solution for 5 min prior to staining with AO (10 μg/ml; Sigma) in SC for 15 min. The sections are rinsed three times in the SC buffer, immersed in 50% ethanol in phosphate-buffered saline (PBS; 0.12 M; pH 7.4) for 2 min, cleared in xylene, and mounted with an antifading medium (Vectashield, Vector Laboratories). To reduce the intense autofluorescence of lipofuscin granules that are abundant in senescent human brain, selected tissue sections can be pretreated with either 0.05% potassium permanganate in PBS for 20 min followed by 0.2% potassium metabisulfite/0.2% oxalic acid in PBS for 30 s (Guntern *et al.*, 1992) or 0.3% Sudan Black B (Sigma; w/vol in 70% ethanol) for 10 min (Yao *et al.*, 2003) prior to AO histochemistry.

B. Microaspiration and LCM

Our laboratory utilizes a Nikon inverted microscope with MetaMorph 5.0 software (Universal Imaging Corporation), an Eppendorf micromanipulator, and an Eppendorf Transjector for single-cell microaspiration. Immunostained or histochemically stained tissue sections are not coverslipped or counterstained and are immersed in RNase-free 0.1 M Tris (pH 7.4) (Ginsberg *et al.*, 1999a, 2000; Hemby *et al.*, 2002, 2003). Individual cells are carefully aspirated from the tissue section and placed in microfuge tubes for subsequent TC RNA amplification. LCM is performed on immunostained or histochemically stained tissue sections that are dehydrated in an ascending series of ethanol and placed in fresh xylenes for a minimum of 15 min. LCM is performed using a PixCell IIe instrument (Arcturus). Caps containing desired captured cells are inverted into a microfuge tube containing Trizol reagent (Invitrogen) prior to initiating TC RNA amplification.

C. Tract-Tracing for Use with Microdissection

Fluorogold (4%; Fluorochrome Inc.) is dissolved in isotonic saline and backfilled into an autoclaved glass micropipette with the tip tapered to ~12–15 μm. FG is iontophoresed into brain regions via 5 μA of current with a 5-s on/off cycle for 10 min. Micropipettes should remain in place 5 min following infusion to allow proper diffusion into the neural tissue

and prevent diffusion up the injection tract. FG is visualized using fluorescence microscopy with fluorescence excitation filter set at 340–380 nm and a barrier filter at 430 nm (Schmued and Heimer, 1990). Microaspiration and LCM are performed on uncoverslipped tissue sections as described above.

D. aRNA Amplification

For aRNA amplification, an oligo d(T)T7 primer (20 ng/μl) is hybridized directly to poly(A)+ mRNAs (Tecott *et al.*, 1988). A double-stranded mRNA–cDNA hybrid is formed by reverse-transcribing the primed mRNAs with dNTPs (1 mM) and 10 U reverse transcriptase (AMVRT, Sekigaku) for 3 h at 42°C (VanGelder *et al.*, 1990). The double-stranded mRNA–cDNA hybrid is converted into double-stranded cDNA by heat denaturing for 5 min at 85°C followed by the addition of dNTPs (1 mM) and 10 U T4 DNA polymerase (Invitrogen) and 10 U Klenow (Invitrogen), forming a functional T7 RNA polymerase promoter. Following the removal of tertiary structures and drop dialyzing the double-stranded cDNA against RNase-free water, the first round of aRNA synthesis occurs using 2000 U T7 RNA polymerase (Epicentre) and NTPs at 37°C for 4 h (Eberwine *et al.*, 2001). The second round of aRNA amplification begins by annealing random hexamers to the newly formed aRNA, and synthesizing a cDNA strand. The oligo d(T)T7 primer is then reintroduced, which binds to the poly(A)+ sequence on the newly synthesized cDNA strand, and a double-stranded cDNA template is formed. aRNA is then tagged with fluorescent, biotinylated, or radiolabeled reagents to enable hybridization to the desired cDNA microarray, oligonucleotide platform, or membrane-based array.

E. TC RNA Amplification

TC RNA amplification consists of immersing microdissected cells or regional dissections in 250 μl of proteinase K solution (50 μg/ml; Ambion) for 12 h at 37°C prior to extraction in Trizol reagent (Invitrogen). RNAs are reverse-transcribed in the presence of the poly d(T) primer (10 ng/μl) and TC primer (10 ng/μl) in 1X first strand buffer (Invitrogen), 1 mM dNTPs, 5 mM dithiothreitol (DTT), 20 U of RNase inhibitor, and 5 U reverse transcriptase (Superscript III; Invitrogen) (Che and Ginsberg, 2004). The synthesized single-stranded cDNAs are converted into double-stranded cDNAs by adding into the reverse transcription reaction the following: 10 mM Tris (pH 8.3), 50 mM KCl, 1.5 mM $MgCl_2$, and 0.5 U RNase H (Invitrogen) in a total volume of 99 μl. Samples are placed in a thermal cycler and second-strand synthesis proceeds as follows: RNase H digestion step 37°C, 10 min; denaturation step 95°C, 3 min, annealing step 50°C, 3 min; elongation step 75°C, 30 min. 5 U (1 μl) *Taq* polymerase (PE Biosystems) is added to the reaction at the initiation of the denaturation step (i.e., hot start) (Che and Ginsberg, 2004). The reaction is terminated with 5 M ammonium

acetate. The samples are extracted in phenol:chloroform:isoamyl alcohol (25:24:1) and ethanol precipitated with 5 μg of linear acrylamide (Ambion) as a carrier. The solution is centrifuged at 14,000 rpm and the pellet is washed once with 95% ethanol and air-dried. The cDNAs are resuspended in 20 μl of RNase-free H_2O and drop dialyzed on 0.025 μm filter membranes (Millipore) against 50 ml of 18.2 MΩ RNase-free H_2O for 2 h. The sample is collected off the dialysis membrane, and hybridization probes are synthesized by IVT using a fluorescent labeling kit (e.g., Cy3 and/or Cy5 labeling; Enzo Life Sciences) as per manufacturer's instructions. Alternatively, hybridization probes can be generated for membrane-based arrays using ^{33}P incorporation in 40 mM Tris (pH 7.5), 7 mM $MgCl_2$, 10 mM NaCl, 2 mM spermidine, 5 mM of DTT, 0.5 mM of ATP, GTP, and CTP, 10 μM of cold UTP, 20 U of RNase inhibitor, 1000 U T7 RNA polymerase (Epicentre), and 40 μCi of ^{33}P-UTP (GE Healthcare) for 4 h at 37°C (Che and Ginsberg, 2004).

F. SELDI-TOF

Patients were diagnosed with ALS by neurological examination using the El Escorial criteria (Brooks, 1994). Postmortem central nervous system tissues from these individuals were obtained from the Division of Neuropathology, Human Brain Resource Center, Johns Hopkins University School of Medicine. Neuropathological evaluation confirmed the clinical diagnosis of ALS (Martin, 1999). The cases studied were sporadic ALS. Postmortem samples of spinal cord from age-matched control individuals without neurological disease ($n = 3$) and patients with ALS ($n = 3$) were selected randomly for analysis.

At autopsy, spinal cord blocks (L5 segment) were dissected and snap-frozen in liquid nitrogen and stored at −80°C. Lumbar spinal cord blocks were sectioned at 12 μm in a cryostat, thaw-mounted onto Superfrost charged glass microscope slides, and stored at −80°C. For LCM, selected slides were stained briefly with Ponceau S prepared in a protease inhibitor cocktail and air-dried. A PixCell II LCM system was used for acquiring motor neurons using a laser spot size of 30 or 60 μm. Motor neuron isolates were lysed with cold 20 mM Tris-HCl (pH = 7.4) containing 10% (wt/vol) sucrose, 20 U/ml aprotinin (trasylol), 20 μg/ml leupeptin, 20 μg/ml antipain, 20 μg/ml pepstatin A, 20 μg/ml chymostatin, 0.1 mM phenylmethylsulfonyl fluoride, 10 mM benzamidine, 1 mM EDTA, and 5 mM EGTA. All of the protease inhibitors were purchased from Sigma. Protein concentration was determined by bicinchoninic acid protein assay kit (Pierce).

PS2 ProteinChip arrays (Ciphergen) were used for SELDI-TOF. PS2 arrays are recommended for use in covalent immobilization of biomolecules for the subsequent capture of target proteins from complex biological samples. PS2 arrays have spots that are preactivated with epoxide chemistry that covalently bind to free primary amine groups on the surface of biomolecules (e.g., antibodies) for immunoassays. The stably immobilized biomolecules

capture proteins from biological samples through specific, noncovalent interactions. The PS2 surface is especially recommended when the aim is to include sensitive detection, low nonspecific binding, and target protein concentrations at less than 1% of total protein.

G. Supplies/Manufacturers

18.2 MΩ RNase-free H_2O (Nanopure Diamond, Barnstead, Dubuque, IA)
AMVRT (Sekigaku, Falmouth, MA)
ATP (Invitrogen, Carlsbad, CA)
Acridine Orange (Sigma, St. Louis, MO)
Ammonium acetate (Sigma)
Antipain (Sigma)
Aprotinin (Sigma)
Bioanalyzer (2100, Agilent Technologies, Palo Alto, CA)
Benzamidine (Sigma)
Chymostatin (Sigma)
Citric acid (Sigma)
Cleaved caspase-3 antibody (Cell Signaling Technology, Beverly, MA)
Caspase-3 active recombinant (Molecular and Biological Laboratories Wobum, MA)
Cresyl violet (Sigma)
dNTPs (Invitrogen)
DTT (Sigma)
EDTA (Sigma)
EGTA (Sigma)
Filter membranes (Millipore, Billerica, MA)
1X First strand buffer (Invitrogen)
Fluorescent labeling kit (Enzo Life Sciences, Farmingdale, NY)
Fluorogold (Fluorochrome Inc., Englewood, CO)
Klenow (Invitrogen)
Leupeptin (Sigma)
Linear acrylamide (Ambion)
MetaMorph 5.0 software (Universal Imaging Corp., Downingtown, PA)
Micromanipulator (Brinkmann-Eppendorf, Westbury, NY)
NTPs (Invitrogen)
Oxalic acid (Sigma)
PALM (PALM Microlaser Technologies, Bernried Germany)
P^{33}-UTP (GE Healthcare, Piscataway, NJ)
PBSII (Ciphergen Biosystems, Fremont, CA)
Pepsatin (Sigma)
Phenol:chloroform:isoamyl alcohol (Invitrogen)
Phenylmethsulfonyl fluoride (Sigma)
PixCell IIe LCM (Arcturus, Mountain View, CA)
Ponceau S (Sigma)
Potassium metabisulfate (Sigma)

Potassium permanganate (Sigma)
Protein assay kit (Pierce, Rockford, IL)
Proteinase K (Ambion, Austin, TX)
Purified mRNAs (Invitrogen)
Reverse transcriptase (Superscript III, Invitrogen)
RNase H (Invitrogen)
RNase inhibitor (Invitrogen)
Spermidine (Sigma)
Sudan Black B (Sigma)
Sucrose (Sigma)
Taq polymerase (PE Biosystems, Foster City, CA)
T4 DNA polymerase (Invitrogen)
T7 RNA polymerase (Epicentre, Madison, WI)
Tris (Sigma)
Trizol reagent (Invitrogen)
UTP (Invitrogen)
Vectasheild (Vector Laboratories, Burlingame, CA)

Acknowledgments. We thank Shaoli Che, M.D., Ph.D., and Scott E. Counts, Ph.D., for their continued efforts on these projects. Support for these projects comes from the NINDS (NS34100, LJM; NS43939, SDG; NS48447, SD6), NIA (AG10668, EJM & SDG; AG14449, EJM & SDG; AG21661, EJM AG05146, LJM; AG16282, LJM), NCI (CA94520; SDG), NIDA (DA013772, SEH; DA013234, SEH), NIMH (MH074313, SEH) and Alzheimer's Association (SDG). We also express our appreciation to the families of the patients studied here, who made this research possible.

REFERENCES

Backes, E., and Hemby, S. E., 2003, Discrete cell gene profiling of ventral tegmental dopamine neurons after acute and chronic cocaine self-administration, *J. Pharmacol. Exp. Ther.* **307:** 450–459.

Bahn, S., Augood, S. J., Ryan, M., Standaert, D. G., Starkey, M., and Emson, P. C., 2001, Gene expression profiling in the post-mortem human brain—no cause for dismay, *J. Chem. Neuroanat.* **22:**79–94.

Barton, A. J. L., Pearson, R. C. A., Najlerahim, A., and Harrison, P. J., 1993, Pre- and postmortem influences on brain RNA, *J. Neurochem.* **61:**1–11.

Becker, I., Becker, K.-F., Röhrl, M. H., Minkus, G., Schütze, K., and Höfler, H., 1996, Single-cell mutation analysis of tumors from stained histologic slides, *Lab. Invest.* **75:**801–807.

Blumberg, D. D., 1987, Creating a ribonuclease-free environment, *Methods Enzymol.* **152:**20–24.

Bonner, R. F., Emmert-Buck, M., Cole, K., Pohida, T., Chuaqui, R., Goldstein, S., and Liotta, L. A., 1997, Laser capture microdissection: molecular analysis of tissue, *Science* **278:**1481–1483.

Brooks, B. R., 1994, El Escorial World Federation of Neurology criteria for the diagnosis of amyotrophic lateral sclerosis, *J. Neurol. Sci.* **124:**96–107.

Brown, P. O., and Botstein, D., 1999, Exploring the new world of the genome with DNA microarrays, *Nat. Genet.* **21**(Suppl):33–37.

Che, S., and Ginsberg, S. D., 2004, Amplification of transcripts using terminal continuation, *Lab. Invest.* **84:**131–137.

Che, S., and Ginsberg, S. D., 2006, RNA amplification methodologies, In: *Progress in RNA Research*, Nova Science Publishing, in press.

Coombs, N. J., Gough, A. C., and Primrose, J. N., 1999, Optimisation of DNA and RNA extraction from archival formalin-fixed tissue, *Nucleic Acids Res.* **27:**e12.

Craven, R. A., Totty, N., Harnden, P., Selby, P. J., and Banks, R. E., 2002, Laser capture microdissection and two-dimensional polyacrylamide gel electrophoresis: evaluation of tissue preparation and sample limitations, *Am. J. Pathol.* **160:**815–822.

Crino, P. B., Khodakhah, K., Becker, K., Ginsberg, S. D., Hemby, S., and Eberwine, J. H., 1998, Presence and phosphorylation of transcription factors in dendrites, *Proc. Natl. Acad. Sci. U.S.A.* **95:**2313–2318.

D'Amore, F., Stribley, J. A., Ohno, T., Wu, G., Wickert, R. S., Delabie, J., Hinrichs, S. H., and Chan, W. C., 1997, Molecular studies on single cells harvested by micromanipulation from archival tissue sections previously stained by immunohistochemistry or nonisotopic *in situ* hybridization, *Lab. Invest.* **76:**219–224.

Dolter, K. E., and Braman, J. C., 2001, Small-sample total RNA purification: laser capture microdissection and cultured cell applications, *Biotechniques* **30:**1358–1361.

Eberwine, J., Kacharmina, J. E., Andrews, C., Miyashiro, K., McIntosh, T., Becker, K., Barrett, T., Hinkle, D., Dent, G., and Marciano, P., 2001, mRNA expression analysis of tissue sections and single cells, *J. Neurosci.* **21:**8310–8314.

Eberwine, J., Yeh, H., Miyashiro, K., Cao, Y., Nair, S., Finnell, R., Zettel, M., and Coleman, P., 1992, Analysis of gene expression in single live neurons, *Proc. Natl. Acad. Sci. U.S.A.* **89:**3010–3014.

Ehrig, T., Abdulkadir, S. A., Dintzis, S. M., Milbrandt, J., and Watson, M. A., 2001, Quantitative amplification of genomic DNA from histological tissue sections after staining with nuclear dyes and laser capture microdissection, *J. Mol. Diagn.* **3:**22–25.

Eisen, M. B., and Brown, P. O., 1999, DNA arrays for analysis of gene expression, *Methods Enzymol.* **303:**179–205.

Emmert-Buck, M. R., Bonner, R. F., Smith, P. D., Chuaqui, R. F., Zhuang, Z., Goldstein, S. R., Weiss, R. A., and Liotta, L. A., 1996, Laser capture microdissection, *Science* **274:**998–1001.

Emsley, J. G., Lu, X., and Hagg, T., 2001, Retrograde tracing techniques influence reported death rates of adult rat nigrostriatal neurons, *Exp. Neurol.* **168:**425–433.

Farrell, R. E., Jr, 1998, *RNA Methodologies*, 2nd edition, San Diego: Academic Press.

Fasulo, W. H., and Hemby, S. E., 2003, Time-dependent changes in gene expression profiles of midbrain dopamine neurons following haloperidol administration, *J. Neurochem.* **87:**205–219.

Fend, F., Emmert-Buck, M. R., Chuaqui, R., Cole, K., Lee, J., Liotta, L. A., and Raffeld, M., 1999, Immuno-LCM: laser capture microdissection of immunostained frozen sections for mRNA analysis, *Am. J. Pathol.* **154:**61–66.

Franklin, T. R., and Druhan, J. P., 2000, The retrograde tracer fluoro-gold interferes with the expression of fos-related antigens, *J. Neurosci. Methods* **98:**1–8.

Freeman, W. M., and Hemby, S. E., 2004, Proteomics for protein expression profiling in neuroscience, *Neurochem. Res.* **29:**1065–1081.

Galvin, J. E., 2004, Neurodegenerative diseases: pathology and the advantage of single-cell profiling, *Neurochem. Res.* **29:**1041–1051.

Galvin, J. E., and Ginsberg, S. D., 2004, Expression profiling and pharmacotherapeutic development in the central nervous system, *Alzheimer Dis. Assoc. Disord.* **18:**264–269.

Ginsberg, S. D., 2001, Gene expression profiling using single cell microdissection combined with cDNA microarrays, In: Geschwind, D. H. (ed.), *DNA Microarrays: The New Frontier in Gene Discovery and Gene Expression Analysis*, Washington: Society for Neuroscience Press, pp. 61–70.

Ginsberg, S. D., and Che, S., 2002, RNA amplification in brain tissues, *Neurochem. Res.* **27:**981–992.

Ginsberg, S. D., and Che, S., 2004, Combined histochemical staining, RNA amplification, regional, and single cell analysis within the hippocampus, *Lab. Invest.* **84:**952–962.

Ginsberg, S. D., and Che, S., 2005, Expression profile analysis within the human hippocampus: comparison of CA1 and CA3 pyramidal neurons, *J. Comp. Neurol.* **487:**107–118.

Ginsberg, S. D., Crino, P. B., Hemby, S. E., Weingarten, J. A., Lee, V. M.-Y., Eberwine, J. H., and Trojanowski, J. Q., 1999a, Predominance of neuronal mRNAs in individual Alzheimer's disease senile plaques, *Ann. Neurol.* **45:**174–181.

Ginsberg, S. D., Crino, P. B., Lee, V. M.-Y., Eberwine, J. H., and Trojanowski, J. Q., 1997, Sequestration of RNA in Alzheimer's disease neurofibrillary tangles and senile plaques, *Ann. Neurol.* **41:**200–209.

Ginsberg, S. D., Elarova, I., Ruben, M., Tan, F., Counts, S. E., Eberwine, J. H., Trojanowski, J. Q., Hemby, S. E., Mufson, E. J., and Che, S., 2004, Single cell gene expression analysis: implications for neurodegenerative and neuropsychiatric disorders, *Neurochem. Res.* **29:**1054–1065.

Ginsberg, S. D., Galvin, J. E., Chiu, T.-S., Lee, V. M.-Y., Masliah, E., and Trojanowski, J. Q., 1998, RNA sequestration to pathological lesions of neurodegenerative disorders, *Acta Neuropathol.* **96:**487–494.

Ginsberg, S. D., Hemby, S. E., Lee, V. M.-Y., Eberwine, J. H., and Trojanowski, J. Q., 2000, Expression profile of transcripts in Alzheimer's disease tangle-bearing CA1 neurons, *Ann. Neurol.* **48:**77–87.

Ginsberg, S. D., Schmidt, M. L., Crino, P. B., Eberwine, J. H., Lee, V. M.-Y., and Trojanowski, J. Q., 1999b, Molecular pathology of Alzheimer's disease and related disorders, In: Peters, A., and Morrison, J. H. (eds.), *Cerebral Cortex, Vol. 14: Neurodegenerative and Age-Related Changes in Structure and Function of Cerebral Cortex*, New York: Kluwer Academic/Plenum, pp. 603–653.

Goldsworthy, S. M., Stockton, P. S., Trempus, C. S., Foley, J. F., and Maronpot, R. R., 1999, Effects of fixation on RNA extraction and amplification from laser capture microdissected tissue, *Mol. Carcinog.* **25:**86–91.

Guntern, R., Bouras, C., Hof, P. R., and Vallet, P. G., 1992, An improved thioflavine S method for staining neurofibrillary tangles and senile plaques in Alzheimer's disease, *Experientia* **48:**8–10.

Hemby, S. E., Ginsberg, S. D., Brunk, B., Arnold, S. E., Trojanowski, J. Q., and Eberwine, J. H., 2002, Gene expression profile for schizophrenia: discrete neuron transcription patterns in the entorhinal cortex, *Arch. Gen. Psychiatry* **59:**631–640.

Hemby, S. E., Trojanowski, J. Q., and Ginsberg, S. D., 2003, Neuron-specific age-related decreases in dopamine receptor subtype mRNAs, *J. Comp. Neurol.* **456:**176–183.

Hynd, M. R., Lewohl, J. M., Scott, H. L., and Dodd, P. R., 2003, Biochemical and molecular studies using human autopsy brain tissue, *J. Neurochem.* **85:**543–562.

Iscove, N. N., Barbara, M., Gu, M., Gibson, M., Modi, C., and Winegarden, N., 2002, Representation is faithfully preserved in global cDNA amplified exponentially from sub-picogram quantities of mRNA, *Nat. Biotechnol.* **20:**940–943.

Issaq, H. J., Veenstra, T. D., Conrads, T. P., and Felschow, D., 2002, The SELDI-TOF MS approach to proteomics: protein profiling and biomarker identification, *Biochem. Biophys. Res. Commun.* **292:**587–592.

Kacharmina, J. E., Crino, P. B., and Eberwine, J., 1999, Preparation of cDNA from single cells and subcellular regions, *Methods Enzymol.* **303:**3–18.

Kamme, F., Salunga, R., Yu, J., Tran, D. T., Zhu, J., Luo, L., Bittner, A., Guo, H. Q., Miller, N., Wan, J., and Erlander, M., 2003, Single-cell microarray analysis in hippocampus CA1: demonstration and validation of cellular heterogeneity, *J. Neurosci.* **23:**3607–3615.

Klur, S., Toy, K., Williams, M. P., and Certa, U., 2004, Evaluation of procedures for amplification of small-size samples for hybridization on microarrays, *Genomics* **83:**508–517.

Kotlyar, M., Fuhrman, S., Ableson, A., and Somogyi, R., 2002, Spearman correlation identifies statistically significant gene expression clusters in spinal cord development and injury, *Neurochem. Res.* **27:**1133–1140.

Lanciego, J. L., and Wouterlood, F. G., 2006, Multiple neuroanatomical tract-tracing, In: Zaborszky, L., Wouterlood, F., and Lanciego, J. L. (eds.), *Neuroanatomical Tract Tracing 3: Molecules-Neurons-Systems*, Springer New York, 336–365.

Lein, E. S., Zhao, X., and Gage, F. H., 2004, Defining a molecular atlas of the hippocampus using DNA microarrays and high-throughput in situ hybridization, *J. Neurosci.* **24:**3879–3889.

Leonard, S., Logel, J., Luthman, D., Casanova, M., Kirch, D., and Freedman, R., 1993, Biological stability of mRNA isolated from human postmortem brain collections, *Biol. Psychiatry.* **33:**456–466.

Lockhart, D. J., Dong, H., Byrne, M. C., Follettie, M. T., Gallo, M. V., Chee, M. S., Mittmann, M., Wang, C., Kobayashi, M., Horton, H., and Brown, E. L., 1996, Expression monitoring by hybridization to high-density oligonucleotide arrays, *Nat. Biotechnol.* **14:**1675–1680.

Lu, L., Neff, F., Dun, Z., Hemmer, B., Oertel, W. H., Schlegel, J., and Hartmann, A., 2004, Gene expression profiles derived from single cells in human postmortem brain, *Brain Res. Brain. Res. Protoc.* **13:**18–25.

Madison, R. D., and Robinson, G. A., 1998, lRNA internal standards quantify sensitivity and amplification efficiency of mammalian gene expression profiling, *Biotechniques* **25:**504–514.

Martin, L. J., 1999, Neuronal death in amyotrophic lateral sclerosis is apoptosis: possible contribution of a programmed cell death mechanism, *J. Neuropathol. Exp. Neurol.* **58:**459–471.

Matz, M., Shagin, D., Bogdanova, E., Britanova, O., Lukyanov, S., Diatchenko, L., and Chenchik, A., 1999, Amplification of cDNA ends based on template-switching effect and step-out PCR, *Nucleic Acids Res.* **27:**1558–1560.

McClain, K. L., Cai, Y.-H., Hicks, J., Peterson, L. E., Yan, X.-T., Che, S., and Ginsberg, S. D., 2005, Expression profiling using human tissues in combination with RNA amplification and microarray analysis: assessment of Langerhans cell histiocytosis, *Amino Acids,* **28:**279–290.

Mikel, U. V., and Becker, R. L., Jr., 1991, A comparative study of quantitative stains for DNA in image cytometry, *Anal. Quant. Cytol. Histol.* **13:**253-260.

Mirnics, K., Middleton, F. A., Marquez, A., Lewis, D. A., and Levitt, P., 2000, Molecular characterization of schizophrenia viewed by microarray analysis of gene expression in prefrontal cortex, *Neuron* **28:**53–67.

Molnar, Z., Blakey, D., Bystron, I., and Carney, R. S. E., 2006, Tract-tracing in developing systems and in post mortem human material using carbocyanine dyes, In: Zaborszky, L., Wouterlood, F., and Lanciego, J. L. (eds.), *Neuroanatomical Tract Tracing 3: Molecules-Neurons-Systems,* New York: Springer, 366–393.

Mouledous, L., Hunt, S., Harcourt, R., Harry, J. L., Williams, K. L., and Gutstein, H. B., 2003, Proteomic analysis of immunostained, laser-capture microdissected brain samples, *Electrophoresis* **24:**296–302.

Mufson, E. J., Counts, S. E., and Ginsberg, S. D., 2002, Single cell gene expression profiles of nucleus basalis cholinergic neurons in Alzheimer's disease, *Neurochem. Res.* **27:**1035–1048.

Mufson, E. J., Ginsberg, S. D., Ikonomovic, M. D., and DeKosky, S. T., 2003, Human cholinergic basal forebrain: chemoanatomy and neurologic dysfunction, *J. Chem. Neuroanat.* **26:**233–242.

Palkovits, M., 1989, Microdissection in combination with biochemical microassays as a tool in tract tracing, In: Heimer, L., and Zaborszky, L. (eds.), *Neuroanatomical Tract Tracing Methods 2: Recent Progress,* New York: Plenum Press, pp. 299–310.

Paweletz, C. P., Liotta, L. A., and Petricoin, E. F., III, 2001, New technologies for biomarker analysis of prostate cancer progression: laser capture microdissection and tissue proteomics, *Urology* **57:**160–163.

Phillips, J., and Eberwine, J. H., 1996, Antisense RNA amplification: a linear amplification method for analyzing the mRNA population from single living cells, *Methods Enzymol. Suppl.* **10:**283–288.

Reiner, A. J., and Honig, M. G., 2006, Dextran amines: versatile tools for anterograde and retrograde studies of nervous system connectivity, In: Zaborszky, L., Wouterlood, F., and Lanciego, J. L. (eds.), *Neuroanatomical Tract Tracing 3: Molecules-Neurons-Systems,* New York: Springer, 304–335.

Sambrook, J., and Russell, D.W., 2001, *Molecular Cloning: A Laboratory Manual, 3rd edition*, Cold Spring Harbor: Cold Spring Harbor Laboratory Press.

Sarnat, H. B., Curry, B., Rewcastle, N. B., and Trevenen, C. L., 1987, Gliosis and glioma distinguished by acridine orange, *Can. J. Neurol. Sci.* **14:**31–35.

Schmued, L. C., and Heimer, L., 1990, Iontophoretic injection of fluoro-gold and other fluorescent tracers, *J. Histochem. Cytochem.* **38:**721–723.

Simone, N. L., Remaley, A. T., Charboneau, L., Petricoin, E. F., 3rd, Glickman, J. W., Emmert-Buck, M. R., Fleisher, T. A., and Liotta, L. A., 2000, Sensitive immunoassay of tissue cell proteins procured by laser capture microdissection, *Am. J. Pathol.* **156:**445–452.

Su, J. M., Perlaky, L., Li, X. N., Leung, H. C., Antalffy, B., Armstrong, D., and Lau, C. C., 2004, Comparison of ethanol versus formalin fixation on preservation of histology and RNA in laser capture microdissected brain tissues, *Brain Pathol.* **14:**175–182.

Suarez-Quian, C. A., Goldstein, S. R., Pohida, T., Smith, P. D., Peterson, J. I., Wellner, E., Ghany, M., and Bonner, R. F., 1999, Laser capture microdissection of single cells from complex tissues, *Biotechniques* **26:**328–335.

Tang, W. X., Fasulo, W. H., Mash, D. C., and Hemby, S. E., 2003, Molecular profiling of midbrain dopamine regions in cocaine overdose victims, *J. Neurochem.* **85:**911–924.

Tecott, L. H., Barchas, J. D., and Eberwine, J. H., 1988, In situ transcription: specific synthesis of complementary DNA in fixed tissue sections, *Science* **240:**1661–1664.

Tkatch, T., Baranauskas, G., and Surmeier, D. J., 2000, Kv4.2 mRNA abundance and A-type K(+) current amplitude are linearly related in basal ganglia and basal forebrain neurons, *J. Neurosci.* **20:**579–588.

To, M. D., Done, S. J., Redston, M., and Andrulis, I. L., 1998, Analysis of mRNA from microdissected frozen tissue sections without RNA isolation, *Am. J. Pathol.* **153:**47–51.

Tomita, H., Vawter, M. P., Walsh, D. M., Evans, S. J., Choudary, P. V., Li, J., Overman, K. M., Atz, M. E., Myers, R. M., Jones, E. G., Watson, S. J., Akil, H., and Bunney W. E. Jr., 2004, Effect of agonal and postmortem factors on gene expression profile: quality control in microarray analyses of postmortem human brain, *Biol. Psychiatry.* **55:**346–352.

Topaloglu, H., and Sarnat, H. B., 1989, Acridine orange-RNA fluorescence maturing neurons in the perinatal rat brain, *Anat. Rec.* **224:**88–93.

Van Deerlin, V. M. D., Ginsberg, S. D., Lee, V. M.-Y., and Trojanowski, J. Q., 2000, Fixed post mortem brain tissue for mRNA expression analysis in neurodegenerative diseases, In: Geschwind, D. H. (ed.), *DNA Microarrays: The New Frontier in Gene Discovery and Gene Expression Analysis*, Washington, DC: Society for Neuroscience, pp. 118–128.

Van Deerlin, V. M. D., Ginsberg, S. D., Lee, V. M.-Y., and Trojanowski, J. Q., 2002, The use of fixed human post mortem brain tissue to study mRNA expression in neurodegenerative diseases: applications of microdissection and mRNA amplification, In: Geschwind, D. H., and Gregg, J. P. (eds.), *Microarrays for the Neurosciences: An Essential Guide*, Boston: MIT Press, pp. 201–235.

VanGelder, R., von Zastrow, M., Yool, A., Dement, W., Barchas, J., and Eberwine, J., 1990, Amplified RNA (aRNA) synthesized from limited quantities of heterogeneous cDNA, *Proc. Natl. Acad. Sci. U.S.A.* **87:**1663–1667.

Vincent, V. A., DeVoss, J. J., Ryan, H. S., and Murphy, G. M., Jr., 2002, Analysis of neuronal gene expression with laser capture microdissection, *J. Neurosci. Res.* **69:**578–586.

von Bertalanffy, L., and Bickis, I., 1956, Identification of cytoplasmic basophilia (ribonucleic acid) by fluorescence microscopy, *J. Histochem. Cytochem.* **4:**481–493.

Wang, E., Miller, L. D., Ohnmacht, G. A., Liu, E. T., and Marincola, F. M., 2000, High-fidelity mRNA amplification for gene profiling, *Nat. Biotechnol.* **18:**457–459.

Yao, P. J., O'Herron, T. M., and Coleman, P. D., 2003, Immunohistochemical characterization of clathrin assembly protein AP180 and synaptophysin in human brain, *Neurobiol. Aging* **24:**173–178.

Zhao, X., Lein, E. S., He, A., Smith, S. C., Aston, C., and Gage, F. H., 2001, Transcriptional profiling reveals strict boundaries between hippocampal subregions, *J. Comp. Neurol.* **441:**187–196.

Zoccarato, F., Cavallini, L., and Alexandre, A., 1999, The pH-sensitive dye acridine orange as a tool to monitor exocytosis/endocytosis in synaptosomes, *J. Neurochem.* **72:**625–633.